Rev. Roum. Sci. Techn.– Électrotechn. et Énerg.
Vol. 71, 3, pp. 445–450, Bucarest, 2026

DUAL-FREQUENCY CONFORMAL SERIES FEED ANTENNA FOR TELEMETRY APPLICATIONS

KANDI RAHARDIYANTI, ANITA PASCAWATI, MIRZA ZULFIKAR RAHMAT, SONNY DWI HARSONO, NURUL FAHRIZATUL ROHMAH, MUH FAKHRI, RACHMAT RAMDANI, BAGUS WICAKSONO, RIKHWANUARY RADITYA PRIYADANA, YUDHA BUDIMAN, RIKA ANDIARTI

Keywords: Series feed network; Conformal antenna; Array; Telemetry.

In this study, a conformal series-feed array antenna for telemetry applications is proposed, operating at 900 MHz and 2.4 GHz. The dual-frequency antenna features a simple geometric design consisting of 5-element and 10-element series-fed arrays, respectively, within a single ground plane, and is fabricated using Roger 5880 material. The proposed antenna was mounted on the cylindrical tube, and various performance parameters were analyzed. The antenna demonstrates reliable dual-band operation, with maximum gains of 7.04 dBi at 930 MHz and 5.85 dBi at 2.46 GHz, along with favorable bandwidth and radiation characteristics. These results highlight the antenna's potential as a compact and effective solution for conformal telemetry systems.

1. INTRODUCTION

An antenna is one of the most fundamental components of wireless communication systems. Antennas are not limited to specific environments or media. They can operate in different media, such as air, water, on the human body, and even on the surface of any radome shape. This versatility allows antennas to be used in a wide range of applications, from satellite communications and wireless networking to medical devices and underground communication systems. For aircraft and rockets, several types of antennas are mounted on the frame or nose cone.

Blade antennas are commonly used and integrated into the aircraft surface. In [1], a blade antenna for UHF aircraft navigation is presented. An aluminum sheet was used as a material to reduce the weight of the antenna and was mounted on a Boeing 777 model. Furthermore, [2] presented a fully steel-made blade antenna for rocket applications and obtained an omnidirectional radiation pattern in a dual configuration of the blade antenna mounted on the rocket chassis. Blade antennas exhibit monopole-like radiation patterns with deep nulls in the upward direction due to their structural similarity to planar monopole antennas, resulting in undesirable blind spots above and below the aircraft in avionic systems [3].

Conformal antennas are increasingly being developed for aircraft applications. Conforming them to the determined shape can improve aircraft aerodynamic drag by adjusting the antenna to the vehicle contour [4]. Previous study [5] showed the advantages of a microstrip conformal antenna, such as broad beam radiation pattern, gain control with the shape, and structural integration, thus improving aerodynamic profiles and requiring no conventional radome. [6] presented a conformal patch antenna for a cargo helicopter belly that resonated at a UHF of 480 MHz, had a peak gain of 6.7 dBi, and was lightweight but had relatively large dimensions. For S-band rocket telemetry, [7] a fabricated conformal array antenna consists of 2 elements, a quarter-wavelength patch using Rogers RT/duroid 5870 PTFE substrate as the material. It had a bandwidth of 37.2 MHz with a maximum gain of 4.37 dBi.

Microstrip antennas are well regarded for their low-profile design. Various methods have been introduced over the past few decades to enhance their performance and enable multifrequency operation. [8] proposed a slot-coupled dipole antenna developed for RFID applications, covering the frequency ranges of 900 MHz and 2.45 GHz. The antenna exhibits a straightforward and symmetrical configuration, providing desirable impedance bandwidth performance with antenna gain ranging from 2.5 to 2.8 dBi in the lower frequency region and 4.5 to 5 dBi in the higher frequency region. For independent port excitation in a dual-band antenna, a two-layer L-probe coupled microstrip patch antenna with integrated shorting vias was proposed [9]. The antenna demonstrates good impedance bandwidth, ranging from 0.78 to 1.02 GHz in the lower band, whereas the measured bandwidth in the upper band ranges from 2.04 to 3.13 GHz. Moreover, microstrip antennas are widely used not only as single elements but also in arrays. Arrays are flexible and are used to create a necessary pattern that a single element cannot achieve [10] (p. 283). Using an array can enhance the performance of the antenna by increasing the gain, beam directivity of the antenna, and other functions that are difficult to produce with a single element [11–13]. Therefore, microstrip antennas are ideal for conformal array applications [14] (p. 1079).

There are three types of feeding of microstrip array antennas: series, corporate, and corporate-series feed network [15]. [16] presented an identical four-element dual-band printed slot antenna fed using a modified 1-to-4 Wilkinson power divider. In [17], an array of 4x4 broadband E-shaped coupling slots for high-speed downlink in small satellites is presented. The corporate feed network with T-junction was used to divide the power signal. In both instances, the feeding methods exhibit a complex nature. A series network, on the other hand, is a simple type of feed network consisting of continuous transmission lines where a portion of the power is fed into each component of an array along the line.

Due to the limited space available on the surfaces of rockets and aircraft, telemetry antennas must be designed in a conformal form that is compact, structurally simple, easy to fabricate, and reliable in performance. Since telemetry systems commonly employ multiple transmitters operating at different frequency bands to enhance operational reliability and support distinct system functions [18,19], independent antenna ports integrated within a shared conformal ground plane are required to enable multi-band and functionally separated communication links under dynamic flight conditions.

In this study, an antenna for telemetry applications was designed to operate in the 900 MHz and 2.4 GHz frequency bands, with two ports integrated on a common ground plane

Research Center for Rocket Technology, National Research and Innovation Agency, Bogor, Indonesia.
E-mails: kand001@brin.go.id, anit005@brin.go.id, mirz002@brin.go.id, sonn001@brin.go.id, nuru035@brin.go.id, muhf002@brin.go.id, rach008@brin.go.id, bagu005@brin.go.id, ikhw001@brin.go.id, yudh002@brin.go.id, rika001@brin.go.id.

DOI : 10.59277/RRST-EE.2026.2.18

substrate. A square patch configuration is adopted to achieve a structurally simple antenna design. Furthermore, the antenna was arranged in an array with a series feed network to increase the gain while retaining its compact shape as well as the ease of its fabrication.

2. ANTENNA DESIGN

The series feed array antenna was designed on a Rogers 5880 substrate with a thickness (h) of 1.6 mm, and the relative dielectric constant (ε_r) of the material is 2.2. The loss tangent ($\tan\,\delta$) of the material is 0.0009. The rectangular patch is the basic element of the series-fed antenna array. This antenna was designed to resonate at 900 MHz and 2.4 GHz, with two different ports on a single substrate. The central element dimension was calculated at 900 MHz and 2.4 GHz according to eq. (1)-(5).

$$W=\frac{c}{2f_o}\sqrt{\frac{2}{\varepsilon_r+1}}\,, \qquad (1)$$

$$\varepsilon_{r,eff}=\frac{\varepsilon_r+1}{2}+\frac{\varepsilon_r-1}{2}\left(1+\frac{12h}{W}\right)^{-\frac{1}{2}}, \qquad (2)$$

$$L_{eff}=\frac{c}{2f_o\sqrt{\varepsilon_{r,eff}}}\,, \qquad (3)$$

$$\Delta L=0.412h\frac{\left(\varepsilon_{r,eff}+0.3\right)\left(\frac{W}{h}+0.264\right)}{\left(\varepsilon_{r,eff}-0.258\right)\left(\frac{W}{h}+0.8\right)}\,, \qquad (4)$$

$$L=L_{eff}-2\Delta L. \qquad (5)$$

The calculated dimensions of the central element patch at a frequency of 900 MHz are L_1 = 110 mm and W_3 = 94 mm, while the dimensions of the central element patch at a frequency of 2.4 GHz are L_a = 43.5 mm and W_e = 38.4 mm. In linear array theory, it is well established that an inter-element spacing of approximately 0.5λ_o is commonly used [20]. Based on these considerations, the inter-element (center-to-center) spacing between adjacent patch elements is set to 124 mm (D) for operation at 900 MHz and 56.5 mm (d) at 2.4 GHz, corresponding to approximately 0.37λ_o and 0.44λ_o, respectively. These spacings are selected to provide a practical compromise between array compactness and radiation performance while maintaining controlled mutual coupling. The microstrip line widths (W_{f1} and W_{fa}) were calculated for a characteristic impedance of 50 Ω for both frequencies. In this array antenna design, the inset feeding technique was used to control the antenna impedance by adjusting the inset gap (w_{s1} and w_{sa}) and inset length (l_{s1} and l_{sa}). The designed antenna is configured to achieve dual-frequency operation, whereby both frequencies are supported within a single common ground plane with an overall dimension of 609×160 mm.

The antenna operates as a five-element linear array at 900 MHz and as a ten-element linear array at 2.4 GHz. The elements are linearly arranged in both frequency bands to maintain a simple geometry and efficient use of space. Patch width variation is employed as an empirical design approach to regulate power extraction and impedance characteristics under compact spacing conditions. The variation is applied from the central elements (W_3 and W_e) toward the outer elements. The outer elements are denoted as W_1, W_2, W_4, and W_5 for the 900 MHz array, and W_a through W_j for the 2.4 GHz array. Figure 1 shows the geometrical configuration of the proposed antenna array operating at frequencies of 900 MHz and 2.4 GHz. Table 1 shows the complete geometrical parameters of the proposed antenna array.

Table 1

The dimensions of the proposed antenna.

Parameter	Dimension [mm]	Parameter	Dimension [mm]
L_1	110	W_d	37.9
L_2	61	W_e	38.4
W_1, W_3	94	W_f	36.7
W_2, W_4, W_5	96	W_g	30.7
W_{f1}	4.3	W_h	23.1
W_{f2}	1.5	W_i	18.5
D	35	W_j	35
l_{s1}	22	W_{fa}	4.8
w_{s1}	1.5	W_{fb}	2.1
L_a	43.5	d	21.1
W_a	17	l_{sa}	10.5
W_b	22.5	w_{sa}	1.6
W_c	31.5		

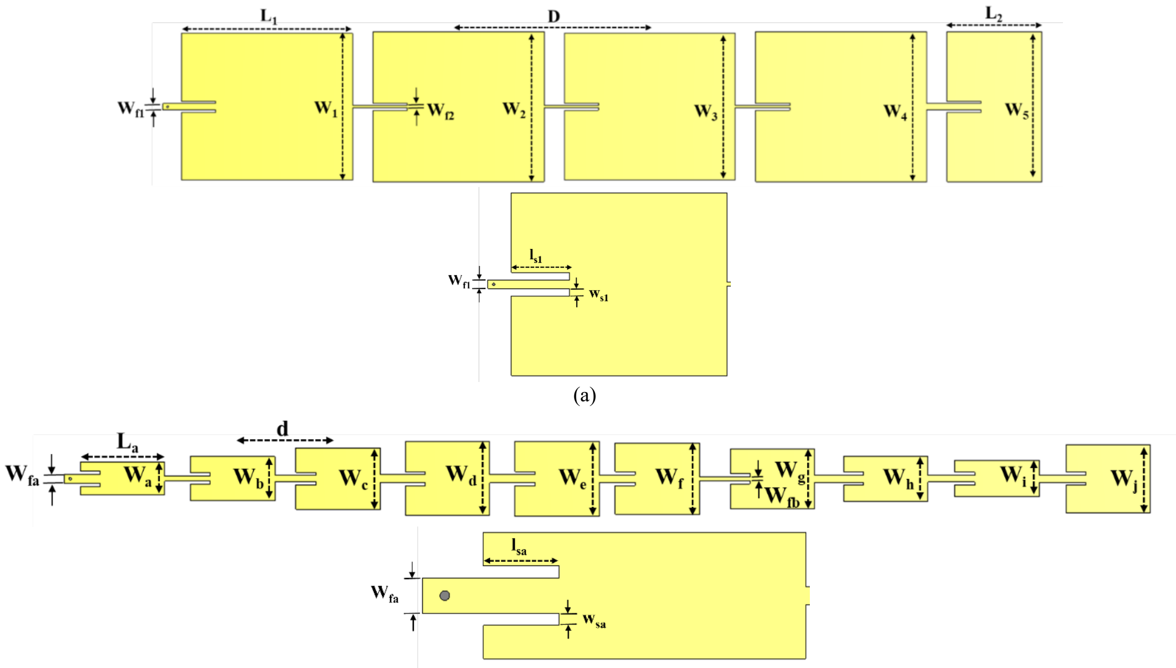

(a)

(b)

Fig. 1 – Array antenna design geometry at frequency; a) 900 MHz; b) 2.4 GHz.

After obtaining the dimensions of the planar array antenna, we conform it to the surface of the telemetry cylinder tube. The height of the telemetry tube is 330 mm with a radius of 195 mm, and the tube thickness is 5 mm. The planar array antenna mounted on the telemetry cylinder tube is illustrated in Fig. 2.

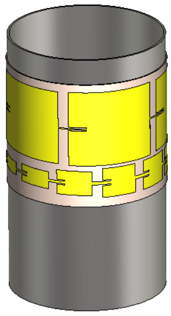

Fig. 2 – The array antenna design mounted on a telemetry cylinder tube.

3. RESULTS AND DISCUSSION

The simulation stage was conducted using the CST Studio Suite. The simulations were first performed for the planar array antenna configuration and subsequently for the conformal array antenna mounted on the telemetry cylinder tube. The evaluated simulation parameters include the return loss (S_{11}), radiation pattern, and gain.

The inset feed affects the antenna design optimization. To determine its influence, simulations are conducted with varying inset feed lengths at both operating frequencies of the antenna. The simulated return loss plots are shown in Fig. 3 with three different values of l_{s1} and l_{sa}. It can be observed from the simulation results that extending the inset feed length tends to enhance the impedance matching performance at a frequency of 900 MHz. In contrast, at 2.4 GHz, it leads to a noticeable frequency shift. However, the best optimization is obtained for antenna configuration where l_{s1} is 22 mm, and l_{sa} is 10.2 mm.

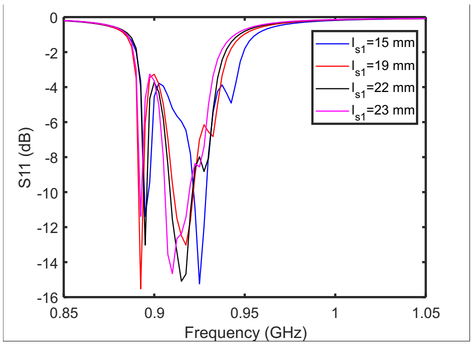

(a)

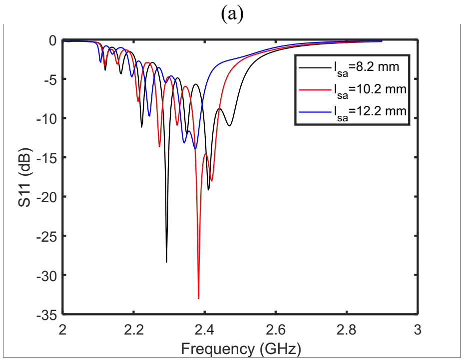

(b)

Fig. 3 – Simulated S_{11} for different lengths of; a) l_{s1}; b) l_{sa}.

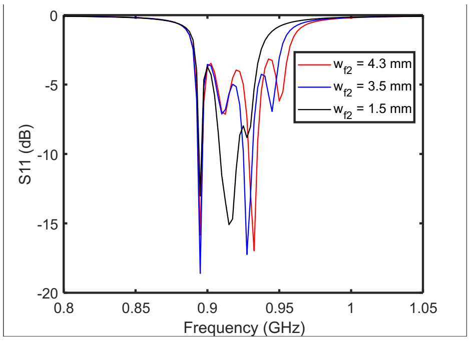

(a)

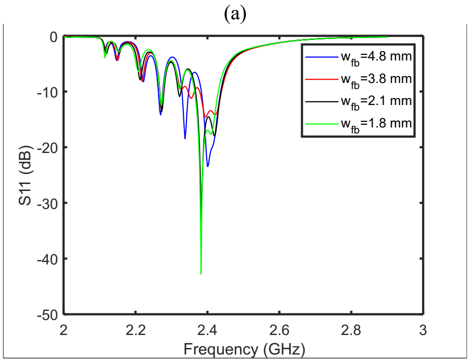

(b)

Fig. 4 – Simulated S_{11} for different widths of: a) W_{f2}; b) W_{fb}.

The effect of the feedline on the matching performance of the antenna was observed by examining the return loss performance for different widths (W_{f1}, W_{f2}, W_{fa}, *and* W_{fb}). For the patch antenna operating at 900 MHz, employing the same parameter values for feedline widths W_{f1} and W_{f2} does not exhibit significant performance optimization. Therefore, optimization is performed by varying the W_{f2} value while keeping W_{f1} fixed at 4.3 mm. The best matching performance is achieved with the antenna configuration where W_{f2} is set to 1.5 mm, as indicated by the return loss value shown in Fig. 4a. Moreover, optimization at 2.4 GHz is achieved through the variation of feedline widths W_{fa} and W_{fb} as the seventh patch element of the antenna structure. In line with the findings at 900 MHz, performance optimization is realized by maintaining a constant width for the feedline of the first patch element (W_{fa}) at 4.8 mm and varying the feedline width W_{fb}. The best impedance matching and bandwidth optimization is achieved by reducing the feedline width W_{fb} to 2.1 mm, as presented in Fig. 4b.

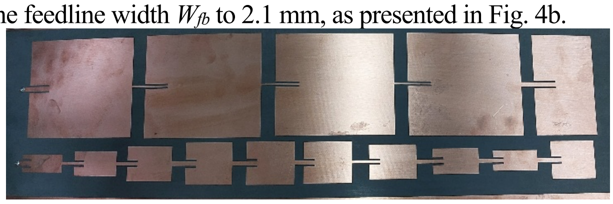

(a)

(b)

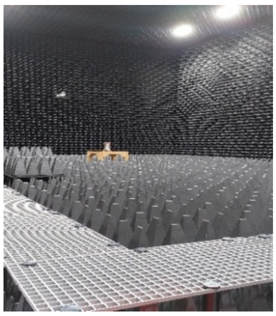

(c)

Fig. 5 – Prototype of proposed antenna: a) antenna with a planar structure; b) proposed antenna mounted on a cylindrical telemetry tube; c) antenna measurement in an anechoic chamber.

Furthermore, the proposed conformal array antenna was fabricated (Fig. 5a), mounted on a cylindrical telemetry tube (Fig. 5b), and subsequently characterized in an anechoic chamber (Fig. 5c). Notably, the cylindrical telemetry tube was precisely abraded to a depth of 1.6 mm to match the antenna thickness. This treatment ensures seamless conformity between the antenna and cylindrical surface, thereby preventing any adverse impact on the aerodynamic performance of the rocket during flight testing.

As shown in Table 2, both simulations and measurements at the two operating frequency bands indicate a reduction in impedance bandwidth when the planar antenna is conformally mounted on a cylindrical structure. Based on the measured results at 900 MHz, the bandwidth decreases from 25 MHz for the planar antenna to 12.85 MHz for the conformal antenna, corresponding to a bandwidth reduction of approximately 48.6%. In contrast, the measured bandwidth was reduced from 95 MHz (planar) to 93.3 MHz (conformal) in the 2.4 GHz band, representing a relatively small decrease of approximately 1.8%. Previous studies have found that bending deformation affects the quality factor of conformal microstrip antennas, leading to a reduction in bandwidth [21,22], particularly at lower frequencies due to the larger electrical size of the antenna.

In addition to the bandwidth variation, a frequency shift between the simulated and measured results was observed for both planar and conformal configurations. In the 900 MHz band, the planar antenna exhibits a slight shift from 922.14 MHz in simulation to 919.5 MHz in measurement, corresponding to a deviation of approximately 0.29%. For the conformal configuration, the center frequency changes from 917.99 to 927.08 MHz, resulting in a shift of approximately 0.99 %.

Similarly, in the 2.4 GHz band, the planar antenna shifts from 2460 to 2447.5 MHz, equivalent to approximately 0.51 %, whereas the conformal antenna shifts from 2420.5 to 2428.15 MHz, corresponding to approximately 0.32 %.

Furthermore, the conformal antenna exhibited a slight frequency shift of approximately 0.82 % at 900 MHz and 0.79 % at 2.4 GHz based on the measurement comparison between planar and conformal configurations. The observed shifts are mainly attributed to bending-induced changes in the effective electrical length of the antenna and the electromagnetic influence of the metallic cylindrical tube used for conformal mounting. The metallic support modifies the boundary conditions and introduces additional loading effects, thereby deviating from the idealized conditions assumed in the simulation model [22–24]. Nevertheless, the measured −10 dB return loss bandwidths in both frequency bands cover the intended operating ranges, confirming the robustness of the proposed conformal antenna design.

Table 2

Comparison of the simulated and measured bandwidths for the planar and conformal antenna configurations.

Frequency band [MHz] (Configuration)	Frequency range [MHz] (Simulation)	Frequency range [MHz] (Measurement)
900 (Planar)	906.56 – 937.71	907 – 932
900 (Confomal)	912.51 – 923.46	920.65 – 933.50
2400 (Planar)	2423 – 2497	2400 – 2495
2400 (Confomal)	2386 – 2455	2381.5 – 2474.8

The isolation between antenna elements, represented by the transmission coefficient (S_{21}), is investigated to assess the level of mutual coupling in the proposed antenna configuration. Fig. 6 shows the measured isolation results for both planar and conformal configurations. At 900 MHz, both configurations exhibit isolation levels better than -30 dB, demonstrating effective suppression of mutual coupling. At 2.4 GHz, although a slight reduction in isolation is observed, the S_{21} values remain below -20 dB. The conformal configuration shows slightly increased coupling compared to the planar case due to the surface curvature effect. Despite this effect, the achieved isolation level remains sufficiently low to satisfy the requirements of practical telemetry applications.

The radiation patterns simulated and measured by the proposed conformal antenna are presented in Fig. 7. After being conformed and mounted on a cylindrical metal tube, the antenna exhibits an omnidirectional radiation characteristic at 900 MHz and provides wide beam coverage at 2.4 GHz. At 900 MHz, the simulated beamwidths are 90.5° in the horizontal plane (ϕ = 0°) and 181.3° in the vertical plane (ϕ = 90°), whereas the measured beamwidths are 80° and 48°, respectively. At 2.4 GHz, the simulated beamwidths are 82.2° in the horizontal plane and 128.6° in the vertical plane, whereas the measured beamwidths are 72° and 44°, respectively. The discrepancy between simulated and measured radiation patterns can be attributed to practical measurement conditions, such as turntable alignment effects, which may distort the measured radiation characteristics in conformal antenna experiments [25]. The presence of a metallic cylindrical considerably impacts the radiation distribution due to induced surface currents and wave reflections, potentially producing multiple maxima lobes and shadow regions in the vertical plane [26]. Although there are discrepancies between the simulation and measurements, both results exhibit comparable overall radiation behavior, particularly in the vertical plane. The antenna maintains wide angular coverage, which is desirable for telemetry applications requiring reliable communication over a broad area of coverage [18,27].

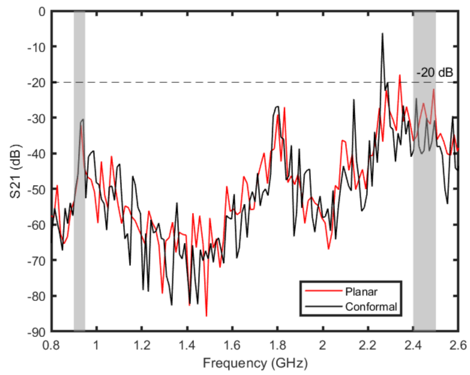

Fig. 6 – Measured isolation (S_{21}) of the proposed antenna for planar and conformal configurations.

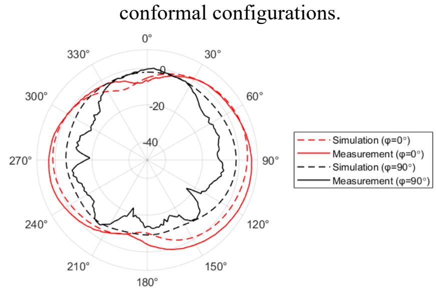

(a)

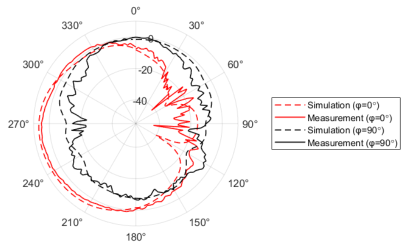

(b)

Fig. 7 – Measured radiation pattern at ϕ = 0º, ϕ = 90º of proposed antenna at; a) 900 MHz; b) 2.4 GHz.

In addition to the beamwidth characteristics, the sidelobe level (SLL) was evaluated at both 900 MHz and 2.4 GHz in the φ = 0° and φ = 90° planes. At 900 MHz, the SLL values ranged from approximately -3 dB to -5 dB for both simulation and measurement results, indicating relatively elevated SLLs. At 2.4 GHz, a lower SLL is observed in the φ = 0° plane (around -20 dB), whereas moderate SLL values of approximately -6 dB appear in the φ = 90° plane. Conventional high-gain phased arrays typically target side lobe levels lower than -10 dB, but the values obtained in this study are consistent with conformal arrays mounted on cylindrical metallic structures [28]. The obtained SLL values represent a trade-off with the wide-beam radiation characteristics of the antenna. Wide angular coverage is preferred over sidelobe suppression for telemetry applications, making the obtained results acceptable for onboard telemetry operations. Furthermore, the proposed conformal antenna achieves a maximum gain of 7.04 dBi at 930 MHz and 5.85 dBi at 2.46 GHz, as presented in Fig. 8.

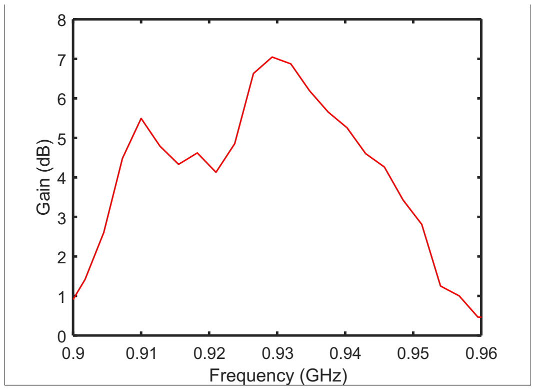

(a)

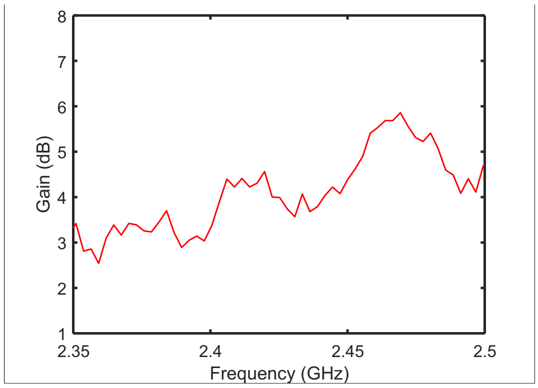

(b)

Fig. 8 – Measured gain of the proposed antenna at frequencies of; a) 900 MHz; b) 2.4 GHz.

Table 3

Summary of comparison between the proposed antenna and prior studies.

Ref.	Frequency (MHz)	Bandwidth (MHz)	Gain (dBi)	Size (mm^2)	Port	Technique used
[6]	480	-	6.7	907.5 x 907.5	Single	Rectangular patch with four edges and styrofoam spacing
[7]	2250	37.2	4.37	-	Single	Quarter-wavelength conformal array
[8]	910; 2450	120; 180	2.8; 5	144 ×13.5	Single	Slot-coupled dipole antenna
[9]	890; 2450	240; 1090	8.4; 8	243.6×243.6	Two-port	L-probe stacked patch supported by shorting vias
This work	900; 2400	12.85; 93.3	7.04; 5.85	609×160	Two-port	Rectangular series feed conformal array

There are limited references in the published literature reporting conformal dual-band antennas with dual-port configurations for telemetry applications. Table 3 presents a comparison of the proposed antenna with previously reported works. Reference [6] presents a conformal antenna designed for helicopter applications. However, it operates at a single frequency and has relatively large dimensions. Reference [7] introduces a compact and simple design, yet it operates at only one frequency. Reference [8] presents a compact antenna *configuration;* however, it is designed for a single port. Reference [9] supports two ports and operates at dual frequencies, but it requires complex fabrication and cannot be conformed to aerial platforms. Therefore, this study proposes a conformal telemetry antenna designed for dual-frequency operation with independent dual ports, featuring a simple geometry that facilitates fabrication while providing high gain performance.

4. **CONCLUSION**

In this study, a dual-band dual-port conformal antenna for telemetry applications operating at 900 MHz and 2.4 GHz was designed and experimentally validated. The antenna maintains stable impedance matching, good port isolation, and wide radiation coverage when mounted on a cylindrical metallic structure, making it suitable for telemetry systems requiring reliable communication across multiple frequency bands. The proposed antenna achieves maximum measured gains of 7.04 dBi at 930 MHz and 5.85 dBi at 2.46 GHz, supporting reliable telemetry links. However, several design trade-offs, including bandwidth reduction and moderate sidelobe levels caused by the structural curvature and the influence of the metallic support, are observed in the conformal implementation. Despite these limitations, the antenna still provides adequate radiation performance for wide-area telemetry coverage. Future work may focus on improving the bandwidth stability under conformal deformation and optimizing the antenna structure to reduce the influence of the metallic platform.

ACKNOWLEDGEMENT

This work was supported by the Government of the Republic of Indonesia under the RIIM-LPDP Research Program Batch 1 Year 2022, Grant No. B-808/II.7.5/FR/6/2022, and B-9546/III.1/KS.00.00/6/2022. The authors wish to extend their sincere appreciation to all staff members of the Telemetry and Control Laboratory, Research Center for Rocket Technology – National Research and Innovation Agency (BRIN), for their valuable cooperation during the antenna fabrication process. Special appreciation is also extended to the technical team of the Anechoic Chamber Laboratory, Research Center for Satellite Technology, for their assistance and support during the antenna measurement activities.

CREDIT AUTHORSHIP CONTRIBUTION STATEMENT

KANDI RAHARDIYANTI: Conceptualization, methodology, antenna design and simulation, formal analysis, writing – original draft.
ANITA PASCAWATI: Investigation and data curation.
MIRZA ZULFIKAR RAHMAT: Result interpretation and writing – review & editing.
SONNY DWI HARSONO: Experimental measurements and writing – review & editing.
NURUL FAHRIZATUL ROHMAH: Data collection and reference management.
MUH FAKHRI: Literature review, project administration, and writing – review & editing.
RACHMAT RAMDANI: Fabrication support and writing – review & editing.
BAGUS WICAKSONO: Drafting figures and writing – review & editing.
RIKHWANUARY RADITYA PRIYADANA: Documentation and writing-review & editing.
YUDHA BUDIMAN: Equipment handling.
RIKA ANDIARTI: Project administration, funding acquisition.

Received on 5 May 2025

REFERENCES

1. N. Saaquib, T. Sarker, N. Rahman, L.E. Khan, P.K. Saha, *Design and development of a wide-band monopole blade antenna for aircraft navigation and communication*, 6th International Conference on Informatics, Electronics and Vision & 7th International Symposium in Computational Medical and Health Technology (ICIEV-ISCMHT), Himeji, Japan, pp. 1–5 (2017).
2. A. Pascawati et al., *Blade antenna 2.4 GHz for rocket applications*, International Conference on Computer System, Information Technology, and Electrical Engineering (COSITE), Banda Aceh, Indonesia, pp. 204–208 (2021).
3. Q. Wu, *Design of a broadband blade and DRA hybrid antenna with hemispherical coverage for wireless communications of UAV swarms*, International Journal of Electronics and Communications, **140**, pp. 1–10 (2021).
4. B. Chauhan, M. Bhatia, A. Chakraborty, P.S. Sharma, A. Sharma, *Cylindrical conformal antenna arrays theory for military aircraft antenna*, IEEE International Conference on Computing, Power and Communication Technologies (GUCON), Greater Noida, India, pp. 77–82 (2020).
5. M.D.C.R. Gonzales, *Analysis of conformal antennas for avionics applications*, Chalmers University of Technology, pp. 1–100 (2007).
6. G.S. Karthikeya, N. Agnihotri, S.S. Siddiq, K.S. Mehul, T. Thyagaraj, *A conformal UHF antenna for cargo helicopter belly*, IEEE 5th Asia-Pacific Conference on Antennas and Propagation (APCAP), Kaohsiung, Taiwan, pp. 285–286 (2016).
7. A. Barton, *Wraparound antenna for S-band telemetry*, U.S. Army Combat Capabilities Development Command Armaments Center, Picatinny Arsenal, New Jersey, pp. 1–10 (2020).
8. T. Mandal, P. Mandal, P. Mondal, L. Murmu, *Design of dual-band monopole antenna for Bluetooth and ultra-wideband with triple notch using electromagnetic bandgap structure*, Rev. Roum. Sci. Techn. – Électrotechn. et Énerg., **67**, *3*, pp. 307–312 (2022).
9. P. Jha, A. Kumar, N. Sharma, *Metamaterial-inspired split ring resonator accomplished multiband antenna for 5G and other wireless applications*, Rev. Roum. Sci. Techn. – Électrotechn. et Énerg., **68**, *2*, pp. 127–131 (2023).
10. P. Sharma, S. Gupta, V.K. Sachan, D. Saxena, *Miniaturized and circular polarized metamaterial-inspired antenna for wireless communication*, Rev. Roum. Sci. Techn. – Électrotechn. et Énerg., **70**, *4*, pp. 525–530 (2025).
11. S. Jeon, Y. Yu, J. Choi, *Dual-band slot-coupled dipole antenna for 900 MHz and 2.45 GHz RFID tag application*, Electronics Letters, **42**, *22*, pp. 1259–1260 (2006).
12. P. Li, K.M. Luk, K.L. Lau, *A dual-feed dual-band L-probe patch antenna*, IEEE Transactions on Antennas and Propagation, **53**, *7*, pp. 2321–2323 (2005).
13. C.A. Balanis, *Antenna theory analysis and design*, John Wiley & Sons, Inc., Hoboken, New Jersey, pp. 1–300 (2005).
14. S.H. Haneef, S.S. Kumar, V. Jayapal, *High gain 2x2 slotted array antenna for 5G mobile applications*, International Journal of Electronics and Telecommunications, **65**, *4*, pp. 557–563 (2018).
15. K.P. Rao, R. Vani, P. Hunagund, *Planar microstrip patch antenna array with gain enhancement*, 8th International Conference on Advances in Computing and Communication (ICACC), Kochi, Kerala, India, pp. 48–57 (2018).
16. L.M. Liya, V.M. Jayakhrisnan, *Enhancement techniques in microstrip patch antenna - a brief review*, 3rd International Conference on Electronics and Sustainable Communication System (ICESC), Coimbatore, India, pp. 367–371 (2022).
17. M.Z. Baba-Ahmed, R.D. Taleb, M.A. Rabah, S. Benabbou, M.I. Soufi, *Hybrid design patch antenna for X-band satellite communication*, Rev. Roum. Sci. Techn. – Électrotechn. et Énerg., **70**, *3*, pp. 376–384 (2025).
18. J.R. James, P.S. Hall, *Handbook of microstrip antennas*, Peter Peregrinus Ltd., London, United Kingdom, pp. 1–200 (1989).
19. H. Errifi, A. Baghdad, A. Badri, A. Sahel, *Design and analysis of directive microstrip patch array antennas with series, corporate and series-corporate feed network*, International Journal of Electronics and Electrical Engineering, **3**, *6*, pp. 416–423 (2015).
20. O. Haraz, M.M.M. Ali, A. Elboushi, A.-R. Sebak, *Four-element dual-band printed slot antenna array for the future 5G mobile communication networks*, IEEE International Symposium on Antennas and Propagation & USNC/URSI National Radio Science Meeting, Vancouver, BC, Canada, pp. 1–2 (2015).
21. K.C. Paul, A. Ahmed, *E-shaped aperture coupled microstrip patch array antenna for high-speed downlink applications in small satellites*, International Journal of Electronics and Telecommunications, **68**, *1*, pp. 47–56 (2022).
22. ***Range Commanders Council, *Telemetry systems radio frequency handbook*, RCC Document 120-21, White Sands Missile Range, New Mexico, USA, pp. 1–100 (2021).
23. A. George, *Design and analysis of 2x2 blade MIMO antenna for UAV communication*, TEQIP III Sponsored International Conference on Microwave Integrated Circuits, Photonics and Wireless Networks (IMICPW), Tiruchirappalli, India, pp. 5–9 (2019).
24. H.L.V. Trees, *Optimum Array Processing Part IV of Detection, Estimation, and Modulation Theory*, John Wiley & Sons, Inc., New York, pp. 1–300 (2002).
25. K. Elleithy, H. Bajwa, A. Elrashidi, *Conformal microstrip printed antenna*, ASEE Northeast Section Conference, University of Hartford, Connecticut, pp. 1–6 (2011).
26. T. Bao et al., *Design of tri-mode frequency reconfigurable UAV conformal antenna based on frequency selection network*, Journal of Low Power Electronics and Applications, **15**, *3*, pp. 1–15 (2025).
27. J. Zhang, J. Huang, P. Sun, F. Meng, J. Zhang, P. Zhao, *Analysis method of bending effect on transmission characteristics of ultra-low-profile rectangular microstrip antenna*, Sensors, **22**, *2*, pp. 1–10 (2022).
28. M.C.R. González, *Analysis of conformal antennas for avionics applications*, Ph.D. dissertation, Department of Signal Theory and Communications, Universidad Carlos III de Madrid, Leganés, Spain, pp. 1–200 (2010).
29. A. Pascawati et al., *Conformal microstrip antennas on the rocket cylinder*, Progress in Electromagnetics Research M, **126**, pp. 1–10 (2024).
30. L. Song, X. Tian, *A wide-beam antenna based on missile telemetry system*, The Applied Computational Electromagnetics Society Journal (ACES), **34**, *5*, pp. 661–668 (2019).
31. Q.Q. He, B.Z. Wang, *Radiation pattern synthesis for a conformal dipole antenna array*, Progress in Electromagnetics Research, **76**, pp. 327–340 (2007)..